Observing downwind structures of urban HCHO plumes from space: Implications to non-methane volatile organic compound emissions

Xiaoxing Zuo[1], Wenfu Sun[2], Isabelle De Smedt[2], Xicheng Li[1], Song Liu[1], Dongchuan Pu[1], Shuai Sun[1], Juan Li[1], Yuyang Chen[1], Weitao Fu[1], Peng zhang[1], Yali Li[1], Xin Yang[1, 3, 4], Tzung-May Fu[1, 3, 4], Huizhong Shen[1, 3, 4], Jianhuai Ye[1, 3, 4], Chen Wang[1, 3, 4], and Lei Zhu[1, 3, 4*]

[1] School of Environmental Science and Engineering, Southern University of Science and Technology, Shenzhen, Guangdong, China.

[2] Division of atmospheric reactive gases, Royal Belgian Institute for Space Aeronomy, Brussels, Belgium.

[3] Guangdong Provincial Observation and Research Station for Coastal Atmosphere and Climate of the Greater Bay Area, Shenzhen, Guangdong, China.

[4] Shenzhen Key Laboratory of Precision Measurement and Early Warning Technology for Urban Environmental Health Risks, School of Environmental Science and Engineering, Southern University of Science and Technology, Shenzhen 518055, China.

* Corresponding to Lei Zhu (zhul3@sustech.edu.cn)

Contents of this file

Figure S1 to S3
Tables S1 to S2
Text S1

Introduction

This Supporting Information provides 3 supplementary figures, 2 supplementary tables, and 1 supplementary text to support the discussions in the main text. The contents of these supplementary materials are as follows.

Observation 1:
Wind out of southeast

(x_0, y_0)

θ

(x_1, y_1)

$$x_1 = x_0 \cos(-\theta) + y_0 \sin(-\theta)$$
$$y_1 = -x_0 \sin(-\theta) + y_0 \cos(-\theta)$$

Observation 2:
Wind out of west

Wind-aligned distribution
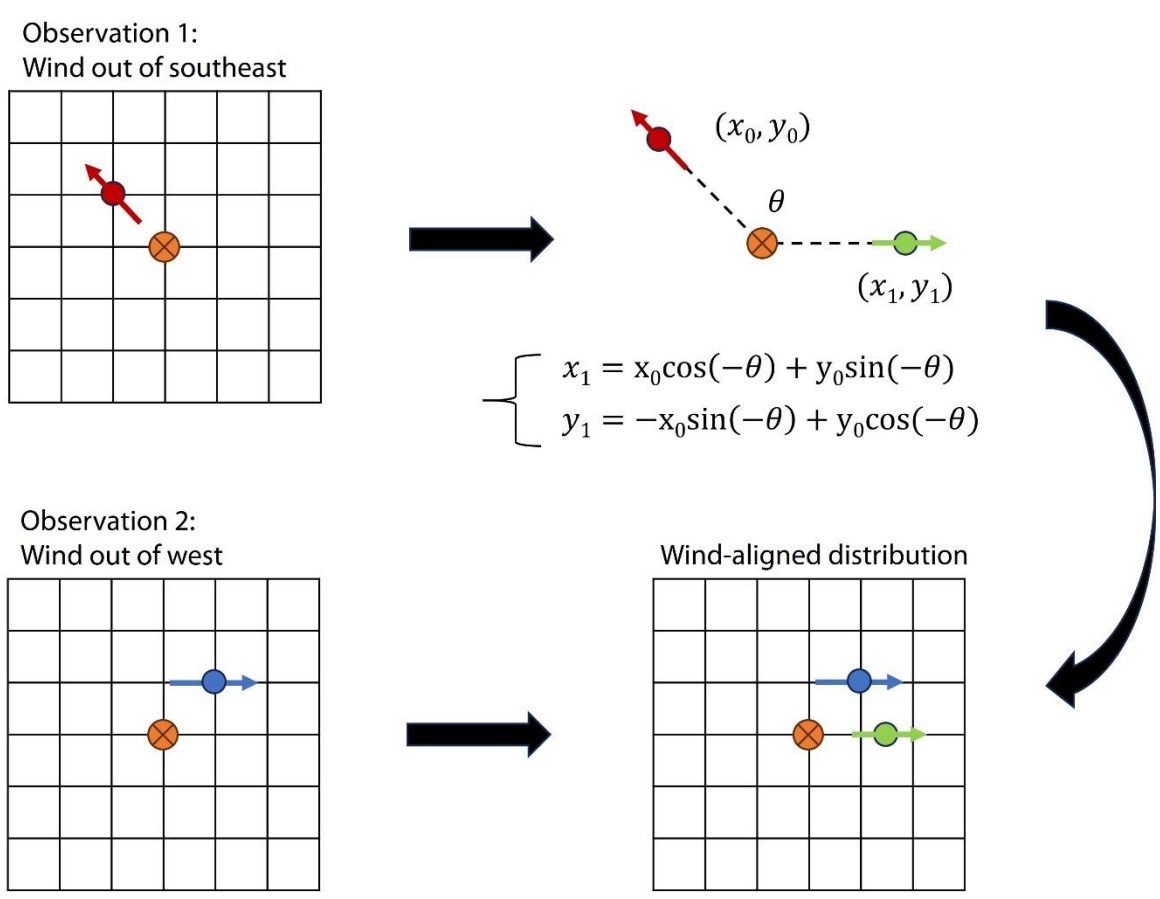
Figure S1. Schematic diagram of wind rotation technique. Each observation is rotated with an angle θ around a reference point (orange dot) to obtain a wind-aligned distribution. Same principle as (Pommier et al., 2013).
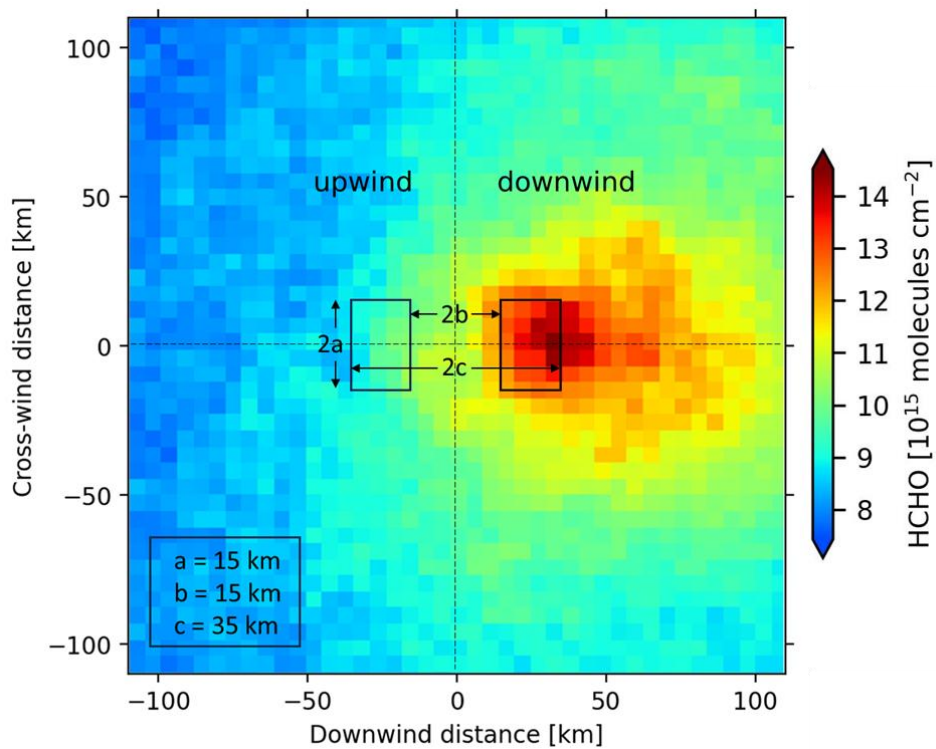
Figure S2. Illustration of signal-to-noise (SNR) ratio method to test a point source.
Data are wind-aligned HCHO columns in Singapore City (a relatively ideal plume). The
two rectangles indicate downwind and upwind averaging regions. a, b, and c are
parameters used in Text S1 (eq. S1). The city center is located at (0 km, 0 km).

(a) Bangkok
(b) Delhi
(c) Dhaka
(d) Esfahan
(e) Ho Chi Minh City
(f) Jakarta
(h) Lagos
(g) Kolkata
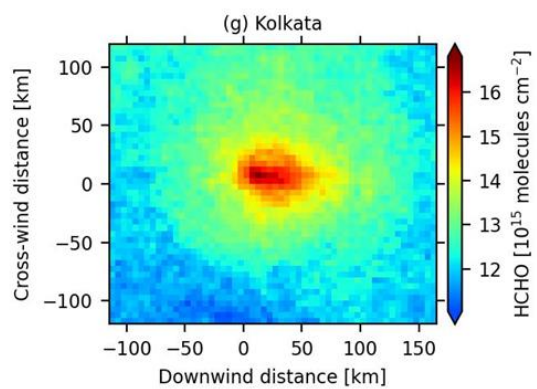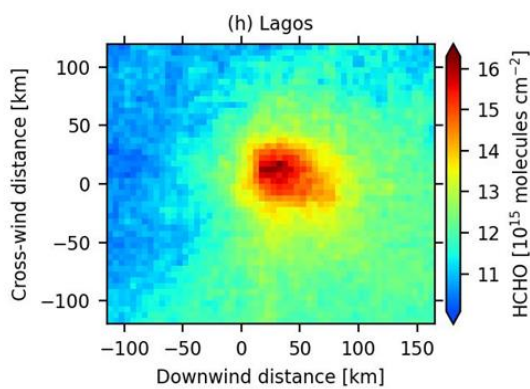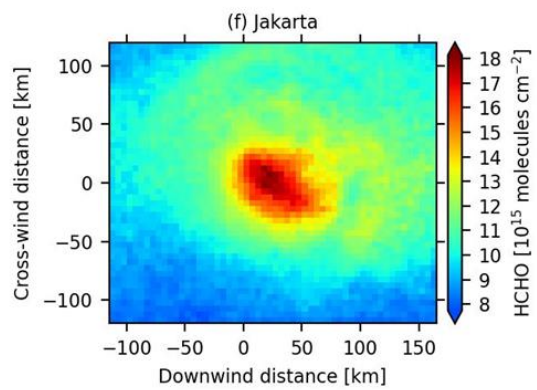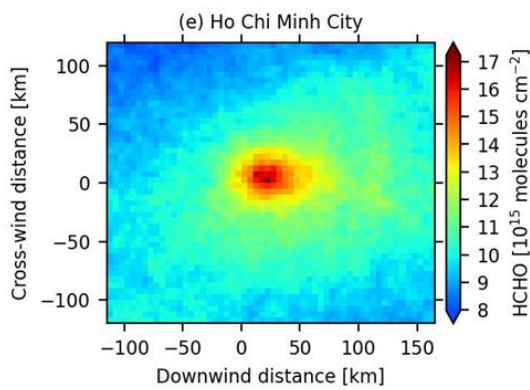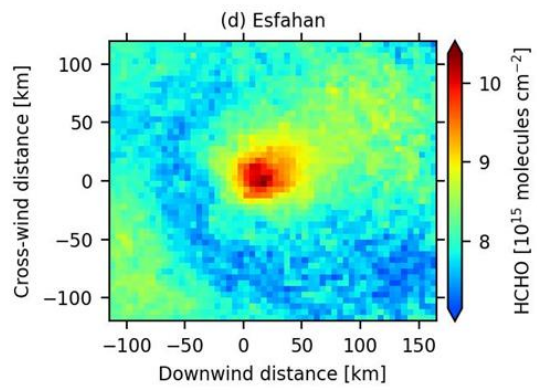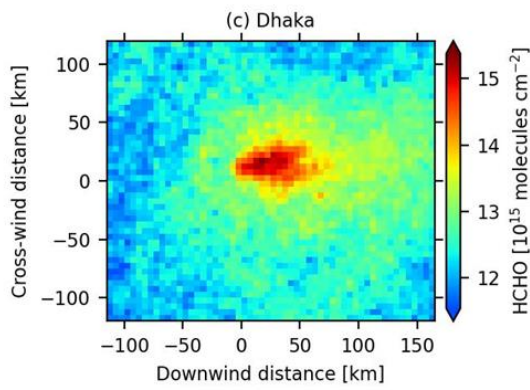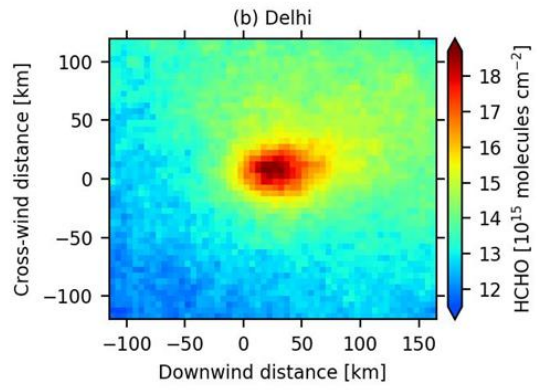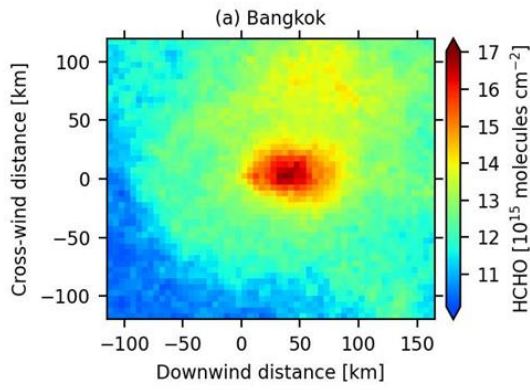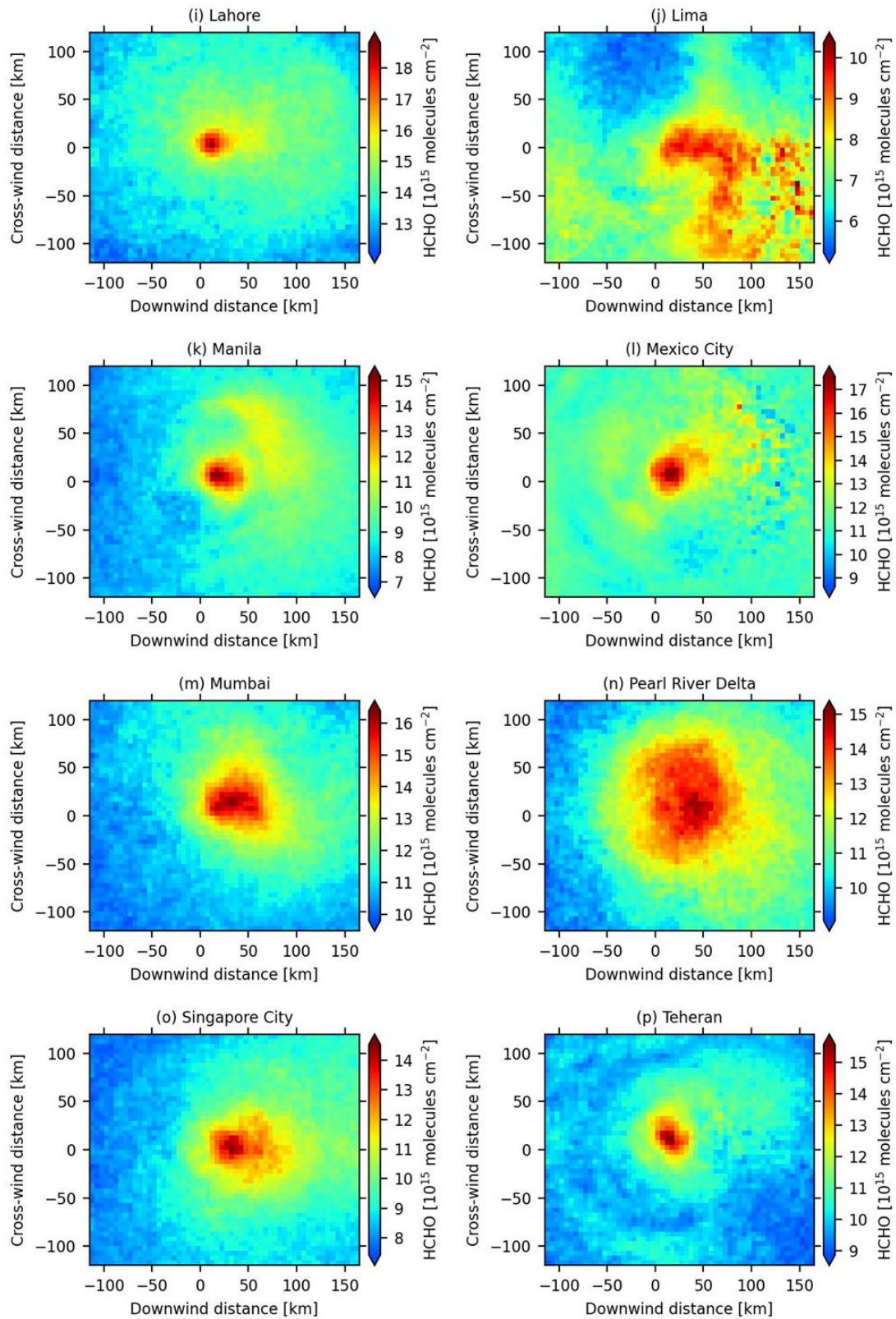
Figure S3. Wind-aligned HCHO columns for 16 cities with valid EMG fitting results.
The panels are labeled the same as in Figure 2.

Table S1. Candidate cities or urban agglomerations. A check mark (√) indicates the criterion is satisfied and a cross mark (×) means not. An asterisk (*) means the city yields a valid fitting with all four criteria fulfilled.

| City	Lat	Lon	Point source criterion	Fitting criterion		
			SNR >10.0 [a]	$R^2>0.8$ [b]	$x_0>\sigma$ [c]	Decay in the domain [d]
Abidjan	5.35	-4.00	×			
Ahmedabad	23.03	72.59	√	√	√	×
Alexandria	31.20	29.92	×			
Baghdad	33.35	44.68	×			
Bangkok *	13.75	100.51	√	√	√	√
Beijing	39.91	116.39	×			
Bengaluru	12.97	77.59	√	√	√	×
Bogota	4.61	-74.08	×			
Busan	35.19	129.10	×			
Cairo	30.05	31.25	×			
Caracas	10.49	-66.88	×			
Chengdu	30.65	104.07	×			
Chongqing	29.56	106.57	×			
Ciudad de Guatemala	14.62	-90.52	×			
Dar es Salaam	-6.82	39.27	√	√	×	√
Delhi *	28.65	77.23	√	√	√	√
Dhaka *	23.71	90.41	√	√	√	√
Dubai	25.08	55.31	×			
Esfahan *	32.65	51.65	√	√	√	√
Hangzhou	30.29	120.16	×			
Hanoi	21.03	105.83	×			
Harbin	45.75	126.65	×			
Hefei	31.86	117.28	×			
Ho Chi Minh City *	10.82	106.63	√	√	√	√
Hyderabad	17.38	78.46	√	√	√	×
Istanbul	41.01	28.95	√	√	√	×
Jakarta *	-6.20	106.83	√	√	√	√
Jeddah	21.50	39.20	√	√	×	√
Johannesburg	-26.20	28.04	×			
Karachi	24.86	67.01	√	√	√	×
Kinshasa	-4.33	15.31	×			
Kolkata *	22.56	88.36	√	√	√	√
Kuala Lumpur	3.14	101.70	×			

City	Lat	Lon	a	b	c	d
Lagos *	6.45	3.39	√	√	√	√
Lahore *	31.56	74.35	√	√	√	√
Lima *	-12.05	-77.04	√	√	√	√
London	51.51	-0.13	✕			
Los Angeles	34.01	-118.25	√	√	✕	√
Manila *	14.60	121.00	√	√	√	√
Mexico City *	19.43	-99.15	√	√	√	√
Milan	45.46	9.19	✕			
Moscow	55.75	37.62	✕			
Mumbai *	19.07	72.89	√	√	√	√
Nanjing	32.06	118.78	✕			
New York	40.71	-74.01	✕			
Osaka	34.69	135.50	✕			
Pearl River Delta *	23.13	113.27	√	√	√	√
Pretoria	-25.75	28.20	✕			
Qingdao	36.06	120.38	✕			
Rio de Janeiro	-22.91	-43.18	✕			
Riyadh	24.67	46.71	√	√	√	✕
Saint Petersburg	59.94	30.31	✕			
Sao Paulo	-23.55	-46.65	✕			
Seoul	37.56	126.98	✕			
Shanghai	31.23	121.49	✕			
Shenyang	41.79	123.43	✕			
Singapore City *	1.37	103.80	√	√	√	√
Suzhou	31.30	120.60	✕			
Sydney	-33.89	151.21	✕			
Taipei	25.05	121.53	✕			
Teheran *	35.70	51.42	√	√	√	√
Tianjin	39.14	117.18	✕			
Tokyo	35.70	139.77	✕			
Urumqi	43.80	87.60	✕			
Wuhan	30.59	114.30	✕			
Xi'an	34.26	108.95	✕			

[a] Signal-to-noise (SNR) approach with a criterion of 10.0 to evaluate the applicability of EMG; [b] $R^2 > 0.8$, which ensures the fitted EMG curve is close to the observations; [c] $x_0 > \sigma$, which requires emission width shorter than the e-folding distance to avoid the case that emission shape confounds with HCHO decay structure; [d] $(150 \text{ km} - \mu) / w > \tau^*$, which states the plume residence time should be longer than the effective HCHO lifetime to reduce EMG fitting uncertainty.

Table S2. EMG-fitted HCHO production rate (*P*), effective HCHO lifetime (τ^*), and background (*B*) for the selected 16 cities or urban agglomerations.

City	EMG-fitted *P* (mol s^{-1})	Uncertainties of *P* (%) [a]	τ^* (h)	Uncertainties of τ^* (%) [b]	*B* (k mol km^{-1})
Bangkok	84.4	52.6%	5.2	52.7%	36.8
Delhi	31.5	50.8%	11.7	32.5%	42.6
Dhaka	14.3	52.2%	13.6	36.8%	40.4
Esfahan	7.0	55.7%	7.8	43.8%	26.1
Ho Chi Minh City	41.9	50.8%	6.7	32.5%	31.8
Jakarta	63.0	50.7%	6.6	32.2%	32.6
Kolkata	48.4	51.1%	4.2	34.6%	40.1
Lagos	34.4	50.8%	11.0	32.9%	36.3
Lahore	15.5	54.0%	17.2	39.2%	44.2
Lima	22.4	55.1%	8.5	53.0%	22.2
Manila	68.6	51.4%	7.3	36.8%	26.0
Mexico City	23.6	57.3%	6.4	53.3%	37.2
Mumbai	52.8	50.3%	5.7	31.6%	35.5
Pearl River Delta	88.5	50.7%	7.3	31.8%	32.0
Singapore City	60.7	50.5%	7.9	32.6%	27.0
Teheran	28.1	50.8%	3.9	33.7%	32.7

[a] Calculated from eq. S1; [b] Calculated from eq. S2

Text S1. Uncertainties in the EMG fitting

The uncertainties of fitted HCHO production rates and effective lifetimes were set as follows:

HCHO tropospheric columns (σ_{VCD}). The uncertainty of TROPOMI HCHO tropospheric columns product is about 50% in remote regions and 25% in elevated column regions (De Smedt et al., 2018) without smoothing error. Since we focus on high-emission regions, we estimate the uncertainty of HCHO columns at 40%. These uncertainties affect the derived HCHO production rates, but not the lifetimes, as they are determined by the relative decay patterns only (Beirle et al., 2011).

Fit errors (σ_{FIT}). We use a confidence interval of 95% as a measure of fitting uncertainty for each location individually.

Choice of wind fields (σ_W). In this study, we used the hourly data on the pressure level of ERA5, using the average of the bottom 5 layers, which is approximately the average wind speed below 1000 m height. The difference in wind speed directly affects the calculation of effective HCHO lifetime and production rate. Referring to previous studies (Beirle et al., 2011; Lee et al., 2022; Lu et al., 2015), we set the uncertainty caused by wind speed at 30%.

The uncertainty of effective HCHO production rate and effective lifetime is calculated as the square root of the sum of squares of the above parts (assuming the various uncertainties to be independent):

$$\sigma_E = E \sqrt{\sigma_{E_{VCD}}^2 + \sigma_{E_{FIT}}^2 + \sigma_{E_W}^2} \tag{S1}$$

$$\sigma_{\tau^*} = \tau \sqrt{\sigma_{\tau^*_{FIT}}^2 + \sigma_{\tau^*_W}^2} \tag{S2}$$

References

Beirle, S., Boersma, K. F., Platt, U., Lawrence, M. G., & Wagner, T. (2011). Megacity Emissions and Lifetimes of Nitrogen Oxides Probed from Space. *Science, 333*(6050), 1737-1739. doi:10.1126/science.1207824

De Smedt, I., Theys, N., Yu, H., Danckaert, T., Lerot, C., Compernolle, S., et al. (2018). Algorithm theoretical baseline for formaldehyde retrievals from S5P TROPOMI and from the QA4ECV project. *Atmospheric Measurement Techniques, 11*(4), 2395-2426. doi:10.5194/amt-11-2395-2018

Lee, T., Wang, Y., & Sun, K. (2022). Impact of Hurricane Ida on Nitrogen Oxide Emissions in Southwestern Louisiana Detected from Space. *Environmental Science & Technology Letters, 9*(10), 808-814. doi:10.1021/acs.estlett.2c00414

Lu, Z., Streets, D. G., de Foy, B., Lamsal, L. N., Duncan, B. N., & Xing, J. (2015). Emissions of nitrogen oxides from US urban areas: estimation from Ozone Monitoring Instrument retrievals for 2005–2014. *Atmospheric Chemistry and Physics, 15*(18), 10367-10383. doi:10.5194/acp-15-10367-2015

Pommier, M., McLinden, C. A., & Deeter, M. (2013). Relative changes in CO emissions over megacities based on observations from space. *Geophysical Research Letters, 40*(14), 3766-3771. doi:10.1002/grl.50704